Effect of fin width ratio on thermal performance of fin based-heat sink with phase change materials

Mustafa Yusuf Yazici[a,b], Mete Avci[c], Orhan Aydin[d], Adeel Arshad[b,e], Mark Jabbal[b]

[a] Department of Mechanical Engineering, Samsun University, 55420, Samsun, Türkiye
[b] Fluids & Thermal Engineering (FLUTE) Research Group, Faculty of Engineering, University of Nottingham, Nottingham NG7 2RD, United Kingdom
[c] Department of Mechanical Engineering, Recep Tayyip Erdogan University, 53100 Rize, Türkiye
[d] Department of Mechanical Engineering, Karadeniz Technical University, 61080, Trabzon, Türkiye
[e] Environment and Sustainability Institute (ESI), Faculty of Environment, Science and Economy, University of Exeter, Penryn Campus, Cornwall, TR10 9FE, United Kingdom.

corresponding author: mustafa.yazici@nottingham.ac.uk

ABSTRACT

The rapid development of electronics, coupled with need of miniaturization in the design and manufacture, makes heat dissipation, which is critical for the performance, lifetime, and reliability of the components extremely challenging. To achieve higher heat dissipation rates, novel fin geometry with variable cross-section considering melting behaviour in medium is presented for PCM-based heat sink beyond previous efforts in literature. In this experimental study, effect of different variable cross-section, which refer different fin width ratio (s=1, 0.5, 0.2 and 0) values are performed on the thermal performance of plate fin-based heat sink with PCM to enhance melting heat transfer. Decreasing fin width ratios point out increasing heat transfer surface area downwardly.-N-eicosane is used. The constant input power is provided at the heat sink base. Thermal performance of novel fin design is evaluated by time-dependent temperature distributions, solid-liquid interface tracking photographs, reliable operating time, enhancement ratio, and thermal conductance. The results reveal that the proposed plate-fin geometry has a significant effect on the cooling performance of PCM-based heat sink.- With the decrease of fin width ratio, higher temperature profile with more uniformity of 52% in the PCM medium, and so lower temperature distribution of 4.5% on the heat sink base are provided. Reliable operating time and thermal conductance values go up 15 % and 38%, respectively, for proposed fin geometry. The improvement on the thermal performance is achieved by the form of the plate-fin, which has increased surface area downward. This provides a great contribution to the conduction and convection heat transfer mechanisms at the lower half of the enclosure. Further, in this study, nearly the same reliable operating time is figured out with proposed fin geometry and fin number of s=0 compared to higher fin number installation of s=1 previously reported.

Keywords: Thermal management, cooling, electronics, heat sink, fin, PCM

NOMENCLATURE

s	:	fin width ratio, s=s1/s2
s1	:	fin top width, mm
s2	:	fin bottom width, mm
t	:	time, minute
θ	:	angular position, º (θ=0 refer vertical position)
Ɛ	:	enhancement ratio
G	:	thermal conductance, W/K
P	:	power, W
T	:	temperature, ºC

1-INTRODUCTION

Development in the electronics industry has come a long way from nascent low-performing devices to advanced devices with high computational speed and power. The advancement in the electronic industry led to an exponential increase in power densities, which in turn simultaneously drove the innovation of smarter and smaller products. The rapid development of electronics, coupled with the need of miniaturization in design and manufacture, make the heat dissipation on the components extremely challenging. If the heat dissipation cannot be effectively dealt with, the resulting overheating problem will cause failures in electrical (slow clock rate, electrical overstress, etc.), mechanical (tensile, fatigue, etc.) and corrosion, and so consequently operation can be interrupted. Therefore, thermal management is becoming critical for the performance, life expectancy, and reliability of electronics components/devices [1-4].

The present era emphasizes the novel thermal management strategies with high heat absorption capability in lesser mass and/or volume, lightweight, and also with silent and no additional power to make reduced carbon footprint electronic devices for a sustainable environment. Phase change material (PCM) based systems offer a very promising thermal management technology with high heat absorption capability, controllable temperature stability, and zero-noise and zero-power consumption [2]. Hence, PCM-based thermal management/cooling systems are used for various applications, especially, which works transiently/intermittent at peak loads, including spacecraft and avionic thermal control [5-6], military equipment (weapon systems, missile electronics etc.) [7-8], power electronics [9], battery thermal management [10-11], light-emitting diodes (LED) [12], PV temperature regulation [13-15], personal computing and communication equipment [16]. PCMs can also be utilised in many other applications and purposes, such as air conditioning systems [17], buildings [18], textile applications [19], and solar thermal applications [20-22]. While PCMs have a great potential to absorb/release excessive heat during the heating/cooling process, they however possess low thermal conductivity, especially organic PCMs. To tackle the low

thermal conductivity issue of PCM, there is interest in the development of heat transfer strategies and thermophysical properties of the PCM including extended surfaces (fin-based), metal/graphite matrix and nano-particles/tubes [23-27]. The addition of an extended surface, also known as a fin, is attractive due to its low cost and ease of manufacturing for heat transfer enhancement and thermal management. Therefore, recent studies on fin-based heat sinks with PCM for electronics cooling, which are related to the present study, are summarized further herein.

Nayak et al. [28] proposed a generalized mathematical formulation and a numerical model to evaluate the thermal performance of PCM-based heat sink with thermal conductivity enhancers: porous matrix, plate and rod-type fins. It is shown that the rod-finned type arrangement achieved a lower hot spot and more uniform temperature distribution on the heat sink base. Kandasamy et al. [29] conducted an experimental and numerical study on a plate fin-based heat sink with PCM. Three types of plate-fin heat sink (small-3 fin, large-6 fin and elliptical) are used in experiments under different constant heat loads. The elliptical plate fin-based heat sink results in lower junction temperature. Results show that PCM-based heat sinks have a great potential for use in intermittent-use devices. Saha et al. [30] experimentally and numerically studied the effects of fin number and thickness on the thermal design of plate-fin-based heat sink with PCM. They found that the base temperature is reduced by decreasing the fin thickness and increasing the fin number. Fok et al. [31] conducted an experimental study on the effects of fin number (3 fins and 6 fins), fin inclination angle and variable load cycles for fin-based heat sink with PCM. They showed that the hot spot temperature is lower with the increase of fin number. Hosseinizadeh et al. [32] performed an experimental study on the thermal behaviour of PCM-based heat sinks with different numbers of plate fins, and fin heights/thickness. They found that an increase in the fin number and fin height led to a significant increase in the overall performance of the system. Various thermal conductivity enhancer (plate-fin, cross-shaped and honeycomb) based heat sink arrangements with different types of PCM materials were investigated experimentally by Mahmoud et al. [33]. They reported that the increase of fin number and inclusion of low melting PCM at moderate power levels significantly extended the reliable operating time of the heat sink. Baby and Balaji [34] performed cooling analyses of various plate/pin fin-based heat sink configurations included PCM. The pin fin arrangement achieved extended operating times compared to the plate-fin. An experimental study on PCM-based heat sinks with various configurations including PCM/silicon matrix, PCM/graphite matrix and plate fins was conducted by Gharbi et al. [35]. It was observed that the PCM/graphite matrix arrangement showed longer operating times than that of the silicon matrix counterpart. Ashraf et al. [36], Arshad et al. [37-39] and Ali et al. [40-41] carried out a series of experimental studies on the thermal performance of pin fin-based heat sink configurations including PCM with various research parameters, namely, pin fin shape (square/round/triangle), dimensional change (thickness and diameter), configuration (staggered and inline array), volume fraction of PCM, and PCM materials. A comparison of the results among the fin geometries showed that the triangular-shaped pin-fins exhibited relatively the best thermal performance. Yazici et al. [42] experimentally studied the combined effects of orientation and the number of fins of a plate fin-based heat sink with PCM. The authors achieved an improvement of 83.4% in operation

time as the inclination angle increased from 0 to 60°. Further, the authors show that the best thermal performance is provided with three fins and 60° angular position. A numerical study was performed to present the effect of natural convection on the thermal performance of a PCM-based heat sink with conventional plate-fin and tree shape conductive structures by Xie et al [43]. Natural convection exhibited positive effects on the heat transfer performance of the PCM-based heat sink and also optimized (using topological optimization) tree shape conductive structure presents a much stronger natural convection to accelerate melting heat transfer. Ho et al. [44] experimentally performed a similar investigation on the heat transfer performance of PCM-based heat sink with different types of thermal conductivity enhancers including plane fin-structure and tree-like structure. Topology-optimized tree-like structure shows reduced wall temperature compared to the fin-structure heat sink. However, the presented heat sink design is based only on optimizing the heat conduction path of the enhanced structure and considering the phase change. The authors do not consider the effects of natural convection during PCM melting in the optimization process. Dammak and El Hami [45] conducted a numerical study on the thermal reliability optimization using Kriging surrogate model of a pin fin heat sink with PCM for electronics cooling. Compared with the referance case, the peak temperature was reduced by 30% for the optimal model. Arshad et al. [46-47] conducted a numerical study to present the effect of the fin thickness fin height and fin volume fraction on the cooling performance of plate fin-based heat sink with PCM. The addition of fins improved the melting of PCM uniformly and more uniform melting is obtained at a fin height of 20 mm and volume fraction of 20%. Kalbasi [48] presented a numerical study on a hybrid plate fin-based heat sink with PCM and air. In this study, the negative effects of PCM volume reduction and the positive effects of heat rejection by the air presence are investigated. Kothari et al. [49] carried out an experimental study to investigate the combined effect of nanoparticle concentration and fin number in plate-fin based- heat sink filled with PCM for electronics cooling. A similar study is also presented by Raj et. al. [50]. Kim et al. [9] reported plate fin-type heat sinks with PCM-integrated base plates where copper matrix phase change composites are included. The PCM-integrated fin-type heat sinks exhibit a lower hot-spot temperature rise until 80 °C in reduced cooling conditions. Jeong et al. [51] investigated the thermal performance of various arrangements of cylindrical heat sinks filled with PCM on the melting process including fin height, cavity angle, fin angle, base thickness, and power level, on PCM for high-power transient cooling. The authors showed that the melting period can be extended by increasing the amount of PCM and increasing the mass of the heat sink material. The authors also reported that the effect of natural convection is enhanced by using large cavity angles. Various research parameters on pin fin-based heat sink with PCM including the number of fins, percentage mass of fins, the shape of fins (prism-triangle/star, Frustrum-triangle/star, inverted Frustrum-triangle/star), and cross-section of fins are investigated numerically by Desai et al [52-53]. It is found that base temperature values obtained for all the prism geometries are lower as compared to all frustum geometries for respective percentage mass of fins [52]. Inverted fins result in lower peak temperature at 25% mass of fins than other configurations [53]. S.Al-Omari et al. [54] proposed a lifted finned heat sink concept (the fins are lifted/unattached from the heat sink base) with PCM. They investigated the effect of sink widths (3.5 cm and 7 cm) and levels of fin detachment (0.5, 1.5, and 2.5 cm). The authors showed that optimized fin lifting can lead to a clear reduction in

peak temperatures and an increase in the rate of heat discharge from the sink. Hemati et al. [55] conducted an experimental study for thermal management of a personal computer power supply unit (PSU) using plate fin-based heat sink with PCM and fan. The results show that increasing the number of fins does not have a favorable effect on the system temperature of the PSU. A combination of passive (PCM) and active (fan) systems provide lower or equal system temperature, reducing in dimensions and the power consumption of the fan.

The above-mentioned literature shows that there are many studies on fin based-heat sink with PCM including number, height, geometry, and arrangement of fins, which takes into consideration only thermal conduction in PCM medium for electronics thermal management. However, research focused on melting natural convection, which enhances solid/liquid phase transition in structural fin design is very scarce in the literature. This reveals the critical research gap for PCM-based heat sink applications. Hence, the motivation of this study is to introduce a novel fin-based heat sink design, which provides a larger heat transfer area at the bottom side based on the melting heat transfer phenomenon/behaviour for higher safe operating time, uniform temperature distribution, and longer product life and so positive impact on environment/economy. This study presents a novel constructal plate-fin design with different fin width ratio (s = 1, 0.5, 0.2 and 0) to enhance conduction and natural convection melting heat transfer mechanisms in the PCM medium for transient electronics cooling. The total heat transfer surface area of fins is kept constant for all width ratio values. The thermal performance of the proposed novel plate fin-based heat sink design filled with PCM is experimentally analysed by plotting transient temperature variation (T)in enclosure/on heat sink base, solid/liquid interface photographing, enhancement ratio (ε) and thermal conductance (G). To evaluate novel plate-finned heat sink geometry, the experimental results are compared with conventional plate fin-based heat sink configuration of the previous study of the authors [42].

2-EXPERIMENTAL STUDY

2.1-Heat storage material

N-eicosane (a type of paraffin-based organic PCM) supplied by Merck Chemicals is used to store dissipated heat from the heat source. Paraffin is known to be an attractive material with its advantages including no phase segregation, chemical/physical/thermal stability, good compatibility with other materials, and non-reactivity, safe and high latent heat of fusion [56]. DSC analysis (Hitachi-DSC 7020) with the temperature accuracy of ±0.1 ºC and calorimeter accuracy of < ± 1%, respectively of pure paraffin is also given in Figure 1. The thermophysical properties of the paraffin are presented in Table 1. Considering the volume expansion (15%) based on the density variation during solid-liquid phase change, 107 g of paraffin is included to the enclosure for all cases.

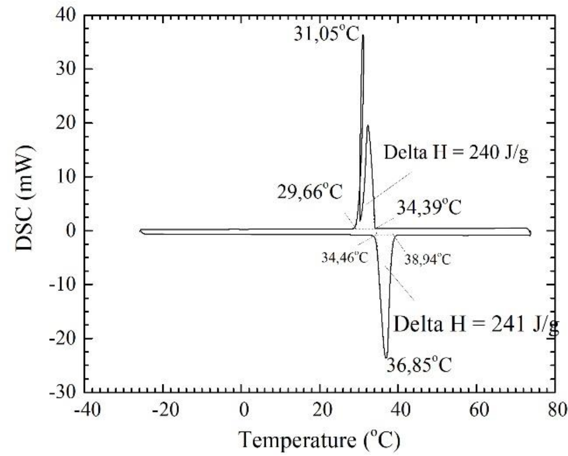

Figure 1. DSC analysis of n-eicosane.

Table 1. Thermo-physical properties of materials [28, 42, 57]

	n-eicosane	Aluminium 6082
Formula	$C_{20}H_{42}$	Al6082
Melting point, ºC	36.85 (± 0.1 ºC)	555
Density, kg/m^3	810 (solid), 770(liquid) (±% 0.2)	2700
Specific heat, kJ/kg.ºC	1.9 (solid), 2.2 (liquid) (< ± 1%)	0.896
Latent heat, kJ/kg	241 (< ± 1%)	-
Thermal conductivity (W/m.K)	0.39 (solid), 0.157 (liquid) (< ±5 %)	172

2.2-Experimental apparatus and procedure

The experimental rig is shown in Figure 2. It consists of a test section, a DC power supply, a data logger, a PC, and also cameras for melting interface visualization.

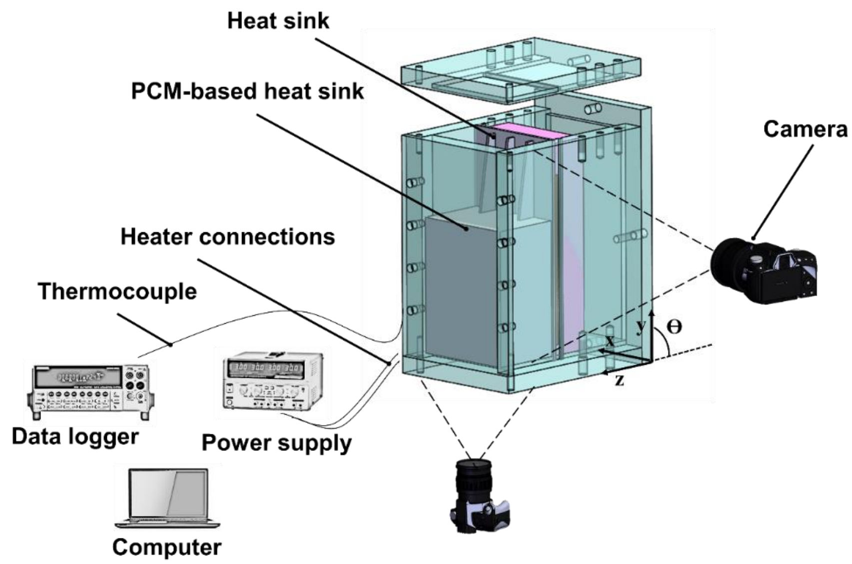

(a)

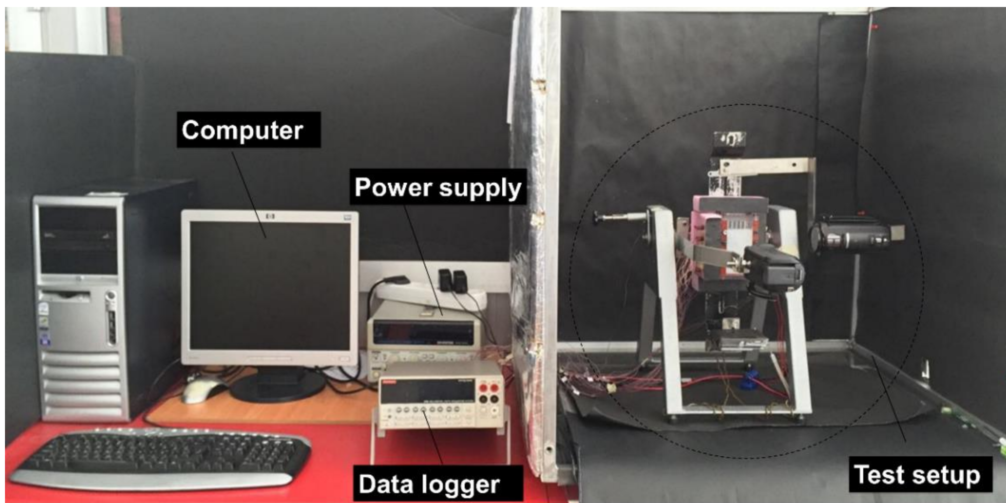

(b)

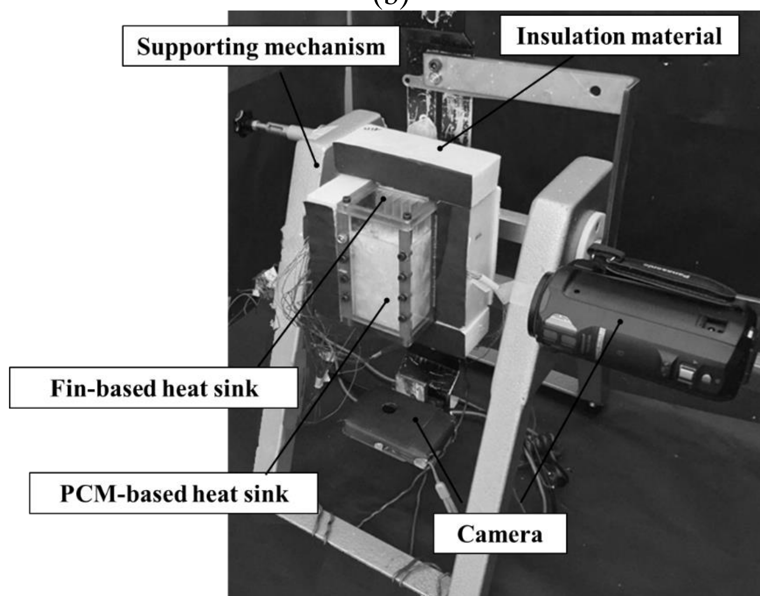

(c)

Figure 2. Experimental rig: (a) schematic model, (b) photograph, and (c) photograph of the test setup

The test section is built to perform the effect of different fin-based heat sink configurations in terms of fin width ratio (s) on the melting phenomenon and so to evaluate thermal response of heating element surface, which mimics the electronic. The test section is an enclosure with inside dimensions of 48 mm in width, 34 mm in depth and 100 mm in height. The test sections are mainly built up with polycarbonate sheets of 10 mm thickness to enable imaging of melting interface tracking. The heat sink part of the test section is machined by EDM (Electrical Discharge Machining) with a thickness of 1.5 mm from aluminum-6082 (k=172 W/m.K), which is used commonly for heat sink material. EDM provides a high precision on dimensions and fine surface quality. The four different fin-based heat sink geometries in terms of fin width ratio ($s= s_1/s_2=1, 0.5, 0.2, 0$) are considered. Technical details of fin-based heat sink configurations are given in Figure 3. Each fin arrangement is 100 mm in height, 1.2 mm in thickness and variable widths of the total heat transfer area of different s values of fins is kept constant. All the geometrical dimensions are measured with accuracy of 0.02mm (0.001 inches) with electronic caliper. The test section is sealed by using sealant elements of high-temperature silicon to avoid leakage. Kapton flexible heater by Omega of dimensions 50mm x 80mm mm is used to mimic heat generation of an electronic component. To provide uniform heat flux at the surface, a 0.2mm thick copper sheet is attached to the heater. The combination of the copper sheet-flexible heater is placed to the base of the heat sink via thermal conducting paste (Omegatherm 201). Electric power of 16 W is supplied through constant/steady current (CC) mode of–DC power supply (GW Instek GPS-4303) with the accuracy of ± 0.01 % (FS). Electric power was calculated practically by constant current and measured voltage. The enclosures are heavily insulated by a 30 mm thick layer of extruded polystyrene board (XPS board) to minimize heat losses to the environment.

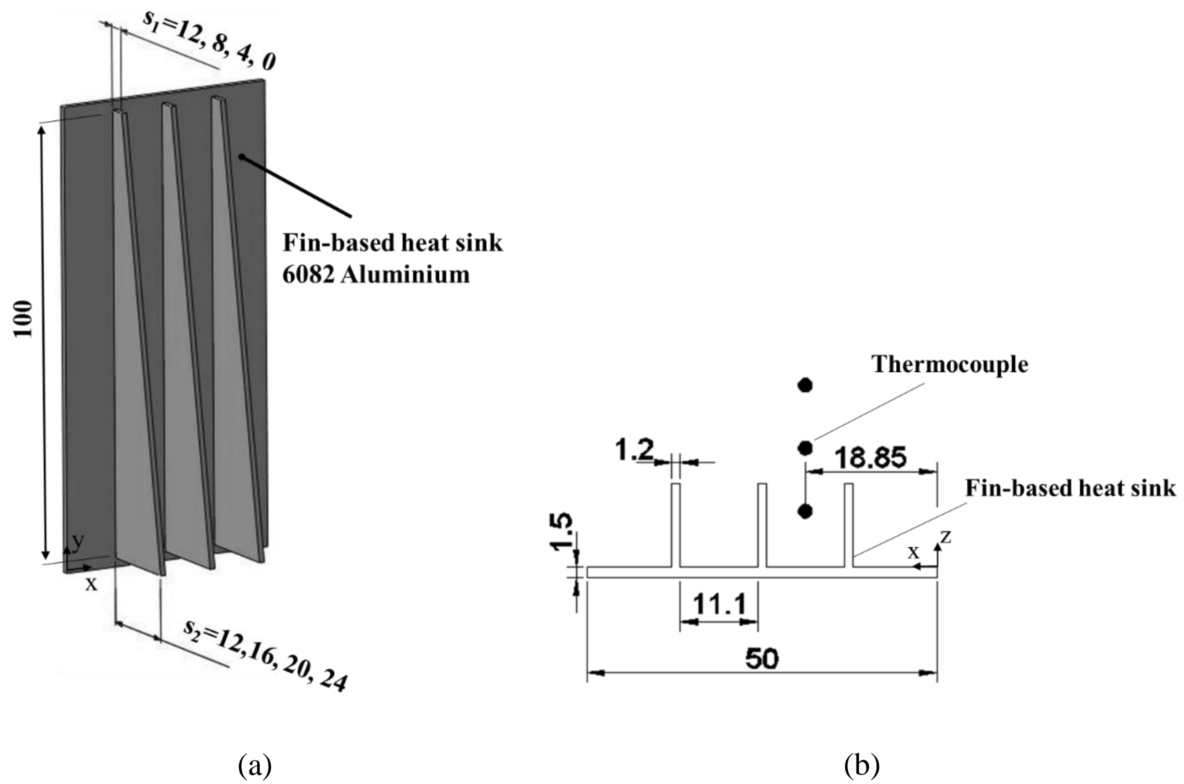

(a) (b)

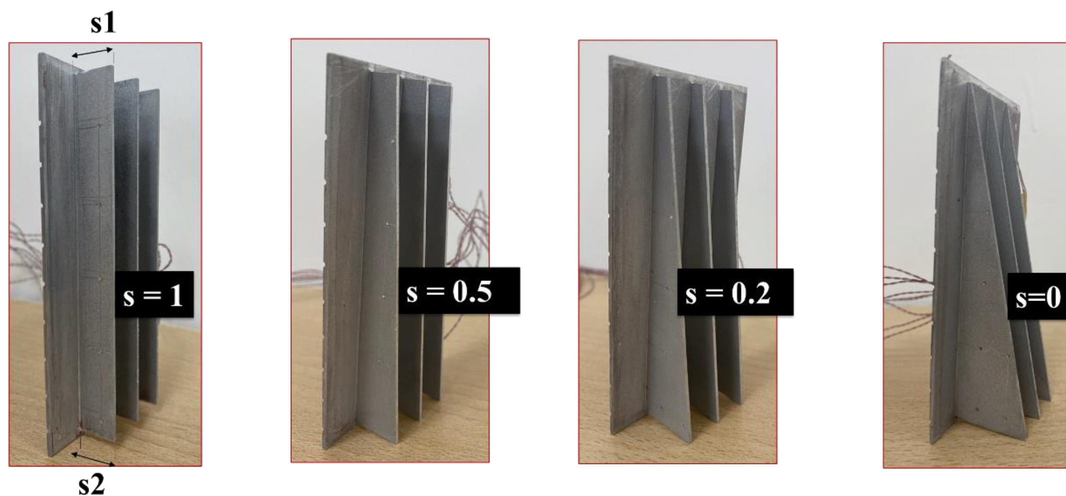

(c)

Figure 3. Schematic view of fin based heat sink: (a) isometric view, (b) overall dimension, and (c) photograph of fin based heat sink configurations (All dimensions are in mm)

To evaluate the thermal performance of heat sink configurations, temperature measurements are taken for both at the heat sink base and in the PCM medium/enclosure. The thermocouple positions/labels at the heat sink base and interior zone are presented in Figure 4. Local temperature points on the heat sink base are measured with nine thermocouples spaced 10 mm apart through the y-axis and on the centre-line of the x-axis. Thermocouples are mounted in the slots of 0.5 mm depth and 1 mm wide so not to disturb the heater placement. The transient

temperature variations in PCM enclosure/medium are achieved with fifteen thermocouples placed between two fins. T-type thermocouples (OMEGA, PFA insulated, 0.25 mm wire diameter) with an accuracy of ±0.5 °C are used and calibrated by constant temperature circulating bath in measuring range of 10 to 100 °C with a discrepancy of ±0.2 °C. The transient temperature recordings are sent to a data logger system (Keithley-2701 with an accuracy of %1) connected to a personal computer, which records the temperatures at ten second intervals.

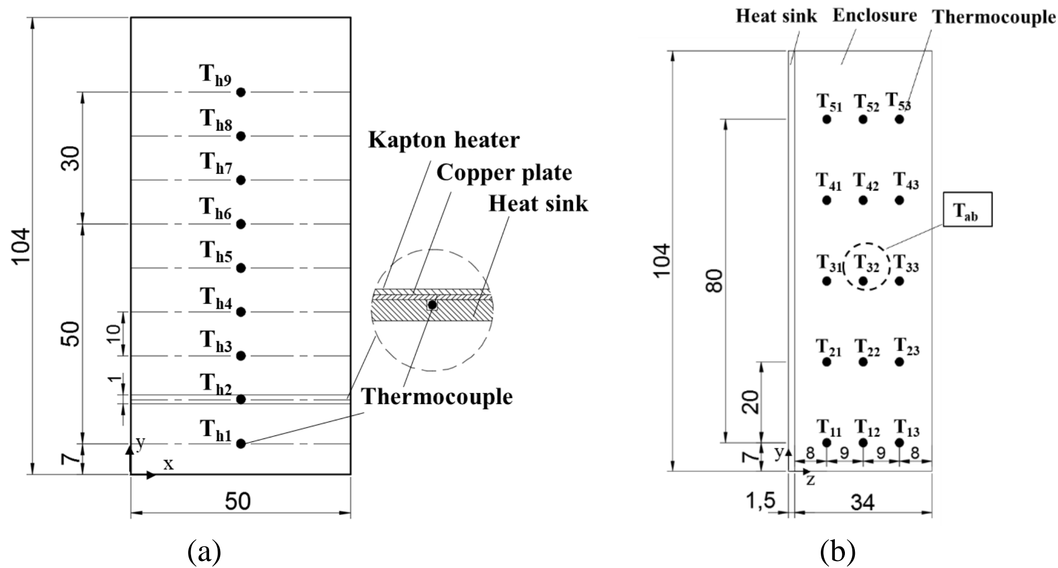

Figure 4. Thermocouple locations and labels: (a) heat sink base, (b) enclosure. (All dimensions are in mm)

To evaluate the effect of different fin-based heat sink configurations on heat transfer mechanisms and melting behaviour, solid-liquid interface progression is also tracked. The time-dependent melting front images from the side and bottom views are captured in three minutes intervals by using two high-resolution digital cameras, which are mounted on the supporting mechanism (Figure 2b). To allow solid-liquid interface imaging, heat-insulating layers (for only side and bottom view) are removed simultaneously about 25 seconds for every 3 minutes.

Experiments are performed in a conditioned room of $T_{ambient}$ = 25 °C. Thermal readings and solid-liquid interface tracking photographs are terminated when the heat sink base temperature reaches 70 °C, which is defined as the reliable operating temperature for electronics components. The transient temperature measurements are found to be repeatable within 2.6-%. The maximum uncertainties in the temperature and heat output are calculated to be ± 2.2 % and ± 3.22 %, respectively, using by Kline and McClintock approach.

3. RESULTS AND DISCUSSION

The present study focuses on a novel plate-fin design considering melting behaviour to provide higher performance, higher lifespan, and positive impact on the green environment for electronics working transiently/periodically/one usage. To evaluate the thermal

performance of the novel plate-finned heat sink configurations with PCM, temperature variation, melting interface photographing, enhancement ratio (ε) and thermal conductance (G) are presented in Figure 5-17 comparatively with conventional plate fin-based heat sink configuration of the previous study of the authors [42].

3.1. Temperature distribution within the PCM medium

The temperature profiles at some specified thermocouple points are presented for different fin width ratios of s in Figures 5-9. Figures 5-8 show the transient temperature variation of the PCM medium at some points on z-planes (horizontal planes) through the height of the enclosure (see Figure 4). The temperature profiles can be divided into 3 stages in the PCM medium: pre-melting, melting and post-melting periods (Figure 5b). Pre-melting period with sensible heat storage presents rapid temperature increment. The melting period with latent heat storage results in a lower temperature increment rate and finally, the temperature profile goes up rapidly into post-melting. It can be noted that solid-liquid phase transition is achieved quickly at the closest point to the heat sink base (T_{a1}). The temperature measurement points closer to the heat sink base have higher temperature values depending on a higher temperature gradient as expected (Figure 5-8). It is seen that temperature curves differ strongly depending on the fin width ratio of s=0.5, 0.2, 0 at the far points from the heat sink base (T_{a2}:T_{12}, T_{22}, T_{32}, T_{42} and T_{a3}: T_{13}, T_{23}, T_{33}, T_{43}) for the lower region of PCM medium (T_{1b}, T_{2b}). The temperature profiles show higher values as the fin width ratio decreases, especially, for T_{a2} and T_{a3} points. For example (at t=40mins), temperature measurements of s = 1,0.5, 0.2 and 0 for T_{2b} (T_{21}, T_{22}, T_{23}) are 53.9 °C, 52 °C, 33 °C; 54 °C, 52.2 °C, 34 °C; 52.9 °C, 51.8 °C, 36 °C; 53 °C, 52.4 °C, 49 °C, respectively, in Figure 6a-d. This is the result of increased extended surface areas at the lower region of the PCM-based heat sink, which provide enhanced conduction heat transfer, and so higher temperature recording. Further, a more uniform temperature distribution is achieved in the lower region of the PCM medium (Figure 5-6) because conductive heat transfer is increased with lower fin width ratio. On the otherside, no appreciable changes (or slight changes) are observed in the upper region of the PCM medium, because the main heat transfer mechanism is melting convection, which circulates hot liquid pcm up and down in terms of temperature dependent density variation (Figure 7-8). It should be noted that the temperature measuring points of T_{5b} (T_{51}, T_{52}, T_{53}) are not in contact with the PCM at the beginning of the melting process due to the amount of PCM based on volumetric expansion. So, T_{5b} temperature points are not shown in the figures.

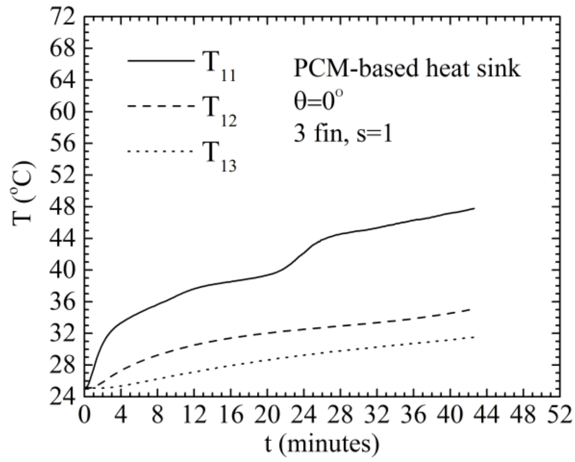

(a)

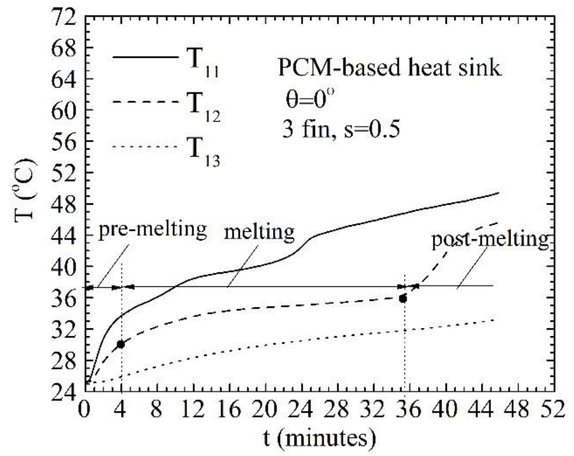

(b)

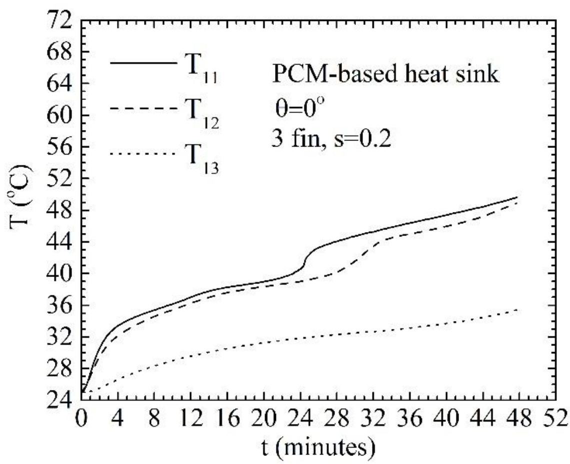

(c)

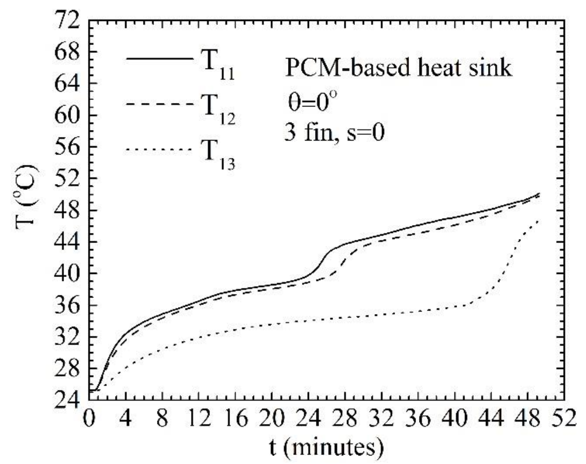

(d)

Figure 5. Time history of the PCM temperature at some specified locations (T_{1b}:T_{11}, T_{12}, T_{13}) at the z plane (horizontal plane): (a) s=1[42], (b) s=0.5, (c) s=0.2, (d) s=0.

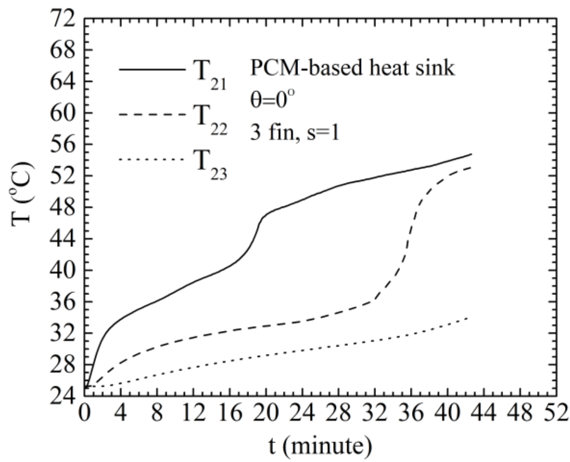

(a)

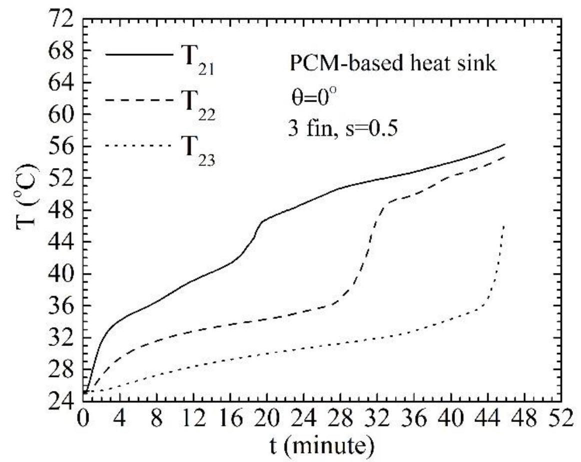

(b)

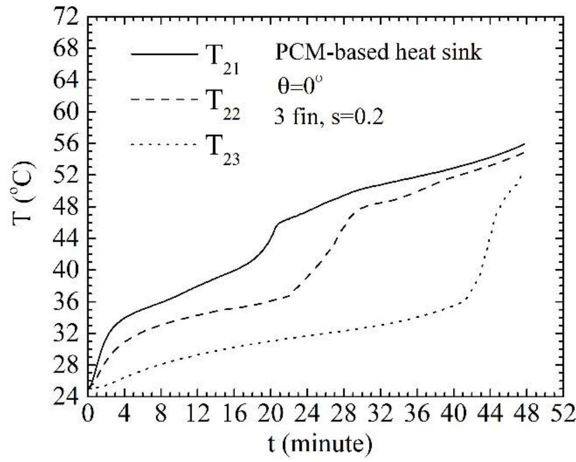

(c)

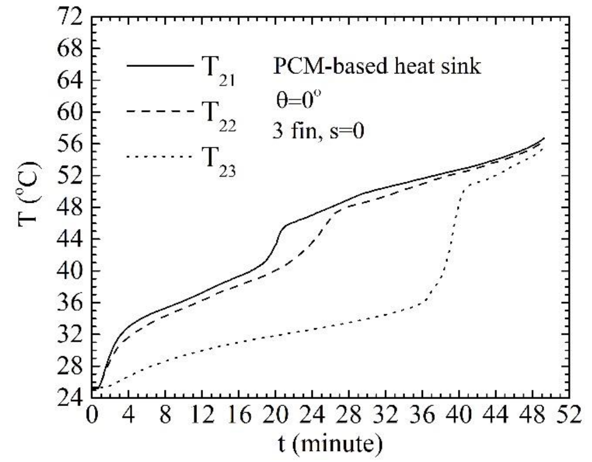

(d)

Figure 6. Time history of the PCM temperature at some specified locations (T_{2b}:T_{21}, T_{22}, T_{23}) z-plane (horizontal plane): (a) s=1[42], (b) s=0.5, (c) s=0.2, (d) s=0.

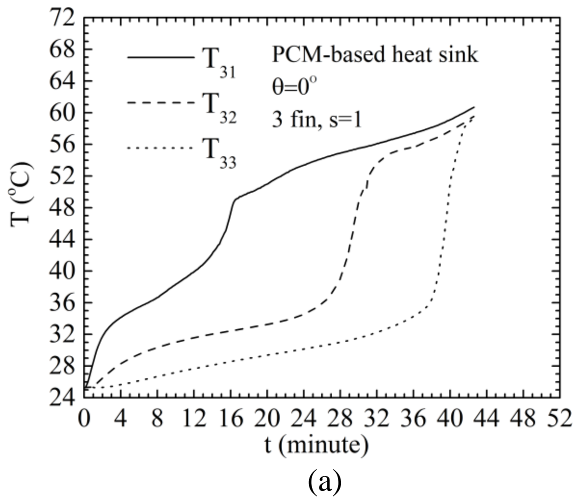

(a)

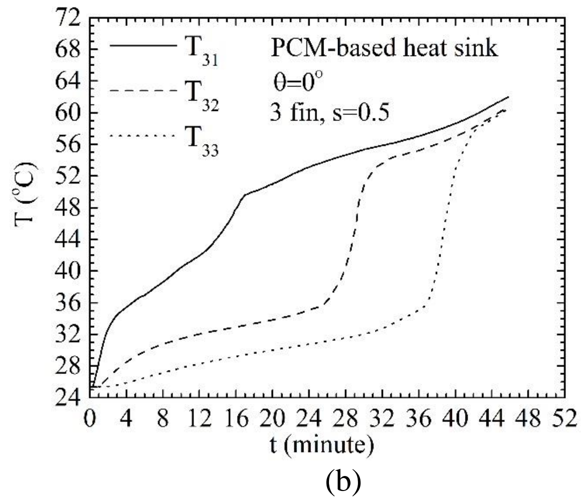

(b)

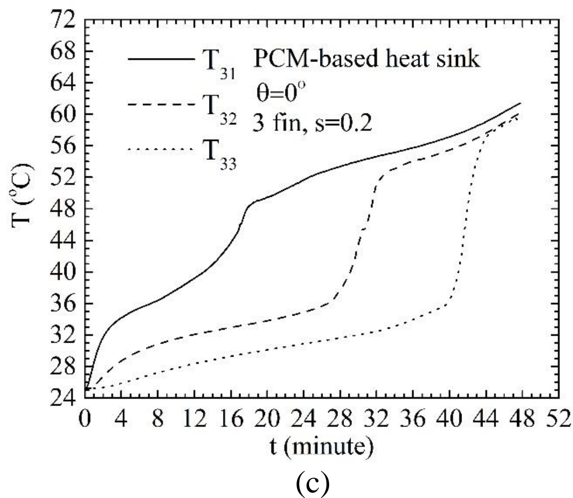

(c)

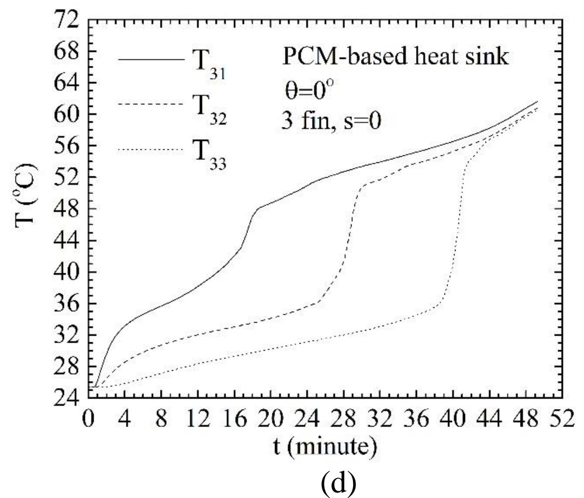

(d)

Figure 7. Time history of the PCM temperature at some specified locations (T_{3b}:T_{31}, T_{32}, T_{33}) z-plane (horizontal plane): (a) s = 1[42], (b) s=0.5, (c) s=0.2, (d) s=0.

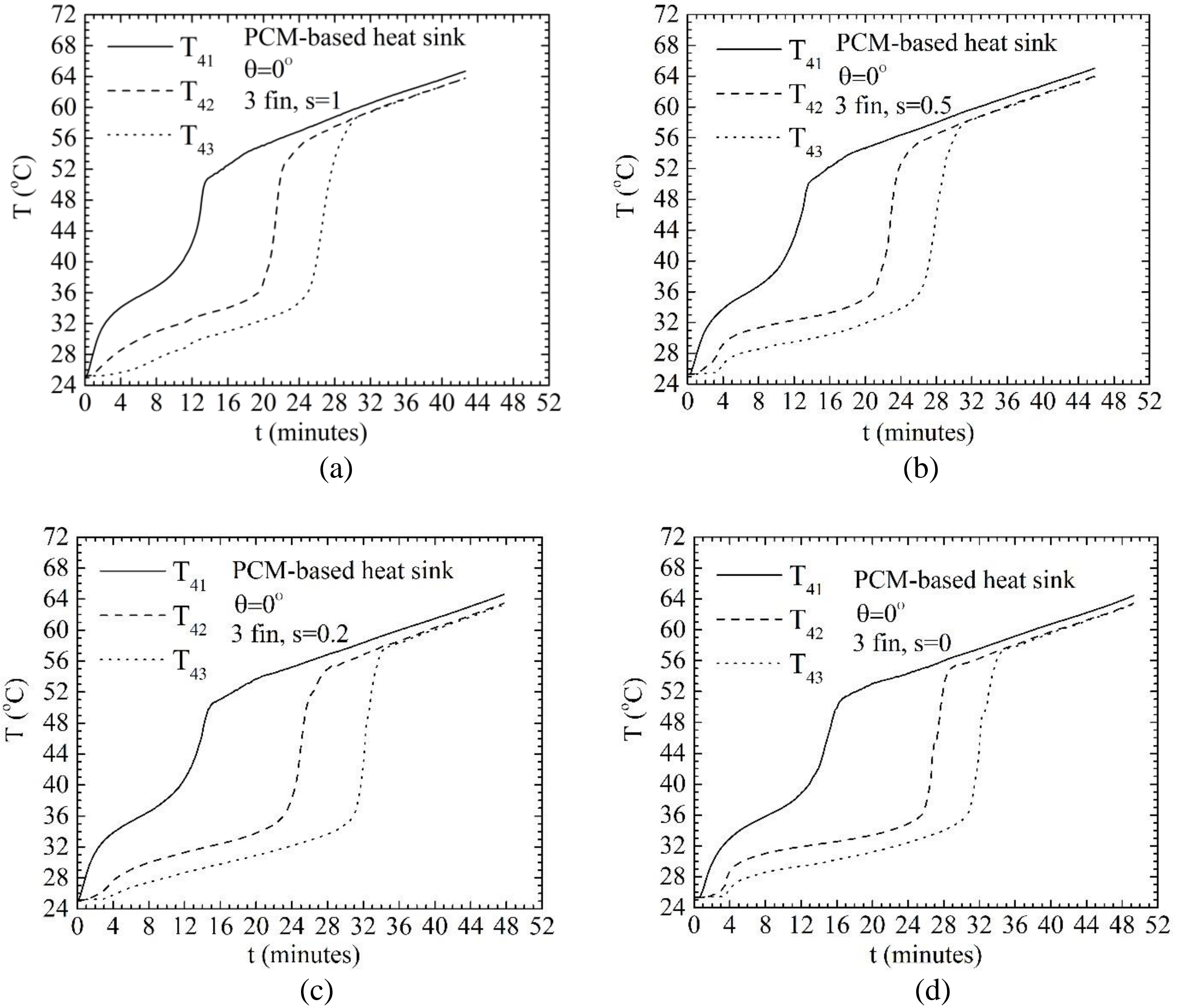

Figure 8. Time history of the PCM temperature at some specified locations (T_{4b}:T_{41}, T_{42}, T_{43}) z-plane (horizontal plane): (a) s=1[42], (b) s=0.5, (c) s=0.2, (d) s=0.

Figure 9 demonstrates the time history of PCM medium temperature at some points through the y-plane (vertical plane) for different s values. The temperature increases in the upper half (T_{3b}, T_{4b}) of the PCM medium compared to the lower half (T_{1b}, T_{2b}). This is because as the liquid fraction increases, melting natural convection intensifies in the melted PCM, which provides a higher contribution of buoyancy forces driving the high-temperature liquid PCM upward. However, it should be noted that at the period of $t<24$-30 minutes in Figure 9 b-d, temperature recordings show a different profile as the s ratio decreases (s = 0.5, 0.2 and 0). This is the result of enhanced heat conduction in the lower part of the PCM medium by increased extended heat transfer surface areas following the melting natural convection phenomenon. To compare the effect of s ratio in the PCM medium, temperature readings at t=40 minutes are given herein for the thermocouple points of T_{a2} (T_{12}, T_{22}, T_{32}, T_{42}). So, readings at T_{a2} are 34 °C, 52 °C, 58 °C, 63 °C; 41,7 °C, 52,2 °C, 57 °C, 61,7 °C; 46 °C, 51,8 °C, 55,5 °C, 60,3 °C; 46,1 °C, 52,4 °C, 55,3 °C, 59,8 °C for s = 1, 0.5, 0.2 and 0, respectively, in Figure 9a-d. These temperature recordings show that lower temperature values at the upper specified thermocouple points and more uniform temperature distribution are achieved in the

PCM medium as the fin width ratio of s decreases. To support the uniformity of the PCM medium, it is seen from Figures 9a and d that the temperature gradients (T_{42} - T_{12}) between the bottom (T_{12}) and top (T_{42}) thermocouple points are reported as 29 °C and 14 °C for s=1 and s=0, respectively. It shows the temperature gradient is decreased by approximately 52% for s=0 compared to the conventional plate fin (s=1). Similarly, this is explained by the enhanced heat conduction mechanism, which is weak in the lower part of the PCM medium, with increasing heat transfer surface area, and the expansion of the convection cells in the downward direction.

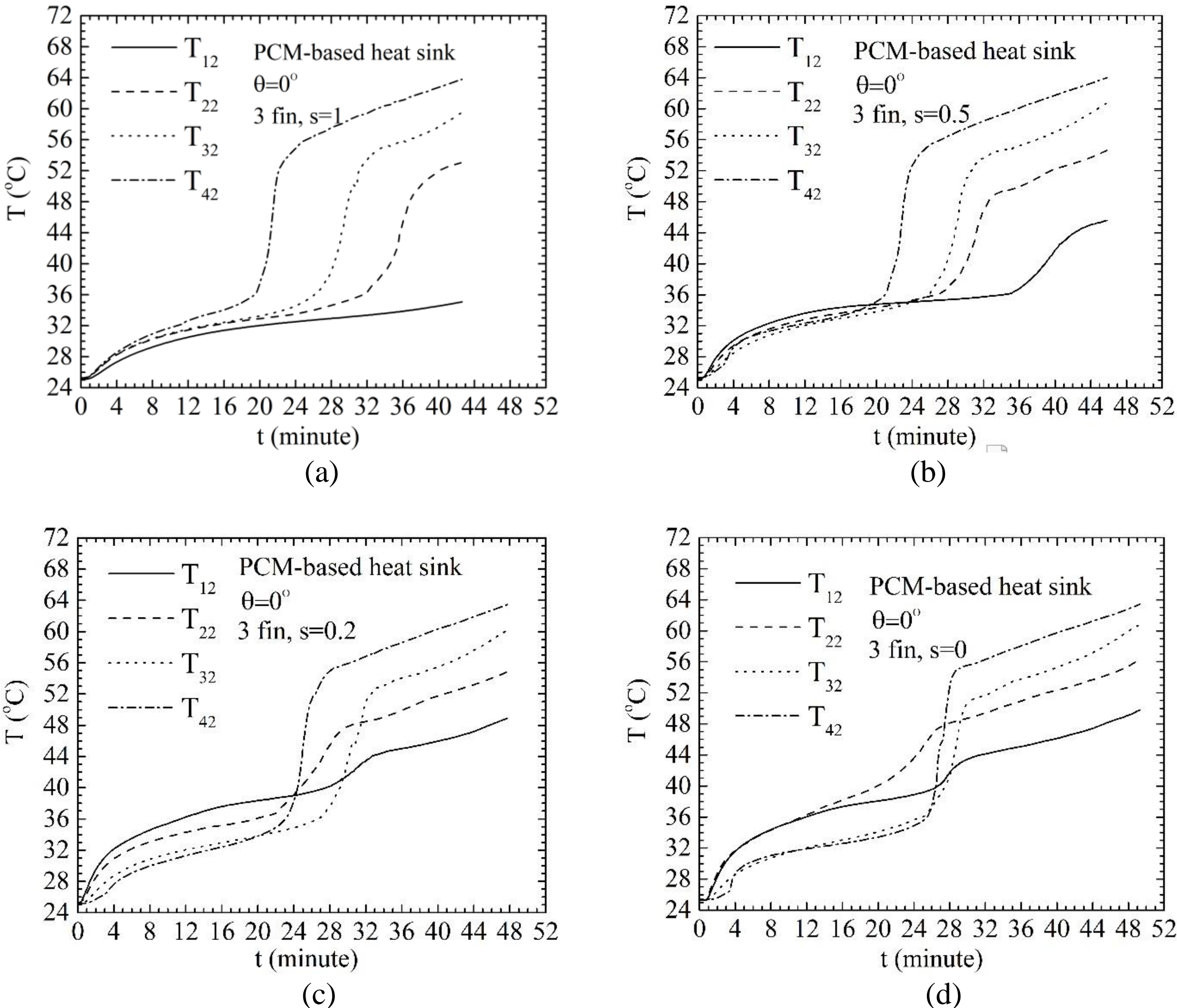

Figure 9. Time history of the PCM medium temperature at some specified locations (T_{a2}:T_{12}, T_{22}, T_{32}, T_{42}) on the y-plane (vertical plane): (a) s=1[42], (b) s=0.5, (c) s=0.2, (d) s=0.

3.2-Temperature distribution on the heat sink base

The transient temperature variations of nine thermocouple points on the heat sink base are depicted for different fin width ratios (s) in Figure 10. It is seen that the base temperature profiles exhibit a similar trend. However, the temperature rising rate diminishes with the decrease of s values (Figure 10b-d). This provides a longer reliable operating time (prolonged time to reach limit operating temperature of 70 °C) and a more uniform temperature distribution on the base surface. The base temperature increases rapidly at the initial stage

(t < 1 minutes), and reaches the melting temperature of the PCM (T_m=35–37 °C). Considering the PCM medium temperature profile (Figure 5-9, t<1 min), it can be seen that the produced heat is stored in the form of sensible heat in the aluminium heat sink with high thermal conductivity and specific heat (c_p), and so the heat is not transferred quickly to the PCM medium, which has a low thermal conductivity coefficient. Hence, at the period of t<1mins, there are no changes in the temperature recordings in the PCM medium (Figure 5-9). At the next stage (1<t<10 mins), as temperature values reach the melting range by absorbing more heat, a thin liquid PCM layer is provided at the base and fin surfaces. This results in an appreciable decrease in temperature rise. The dominant heat transfer mechanism in this period (1<t<10/12 mins) is conduction due to weaker buoyancy forces compared to the viscous forces. As time elapses (t>10/12 mins), the liquid fraction expands. This makes stronger buoyancy forces and so stronger convective cells in the PCM medium. These provide lower temperature increases in this period compared to the previous stage. Melting convection is the dominant heat transfer mechanism in this period. To compare the effect of s ratio, for example (at t = 40 mins), the critical (or maximum) temperature point recordings of s = 1, 0.5, 0.2 and 0 are reported 70 °C, 68.7 °C, 68 °C and 67 °C, respectively. It means 4.5% lower temperature is achieved for s=0 compared to conventional plate fin of s=1. To evaluate thermal stress on the heat sink base, it should be noted that maximum temperature difference ($\Delta T_{max} = T_{hmax} - T_{h1}$) is reduced by 1.1 °C for s=0 (ΔT_{max} = 10 °C) compared to s=1 (ΔT_{max} = 11 °C). In addition, it is shown in Figures 10 a-d that the critical temperature point changes downward as T_{h7} for s = 0. This is explained by the rapid solid-liquid phase transition via enhanced conduction and expanded convection cells at the lower half of the enclosure.

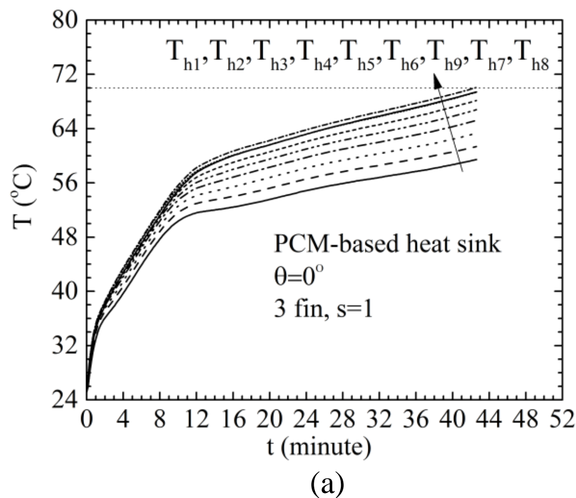

(a)

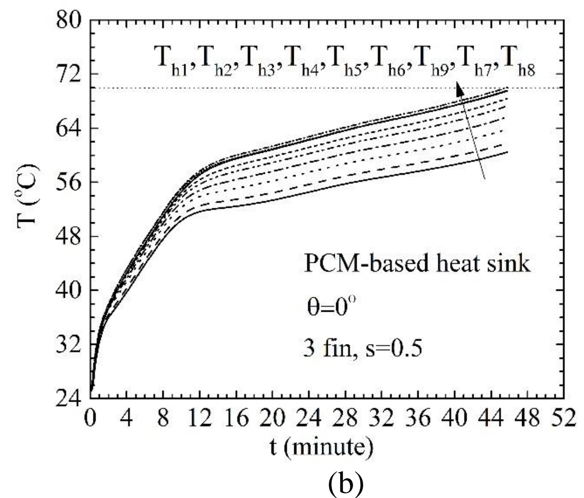

(b)

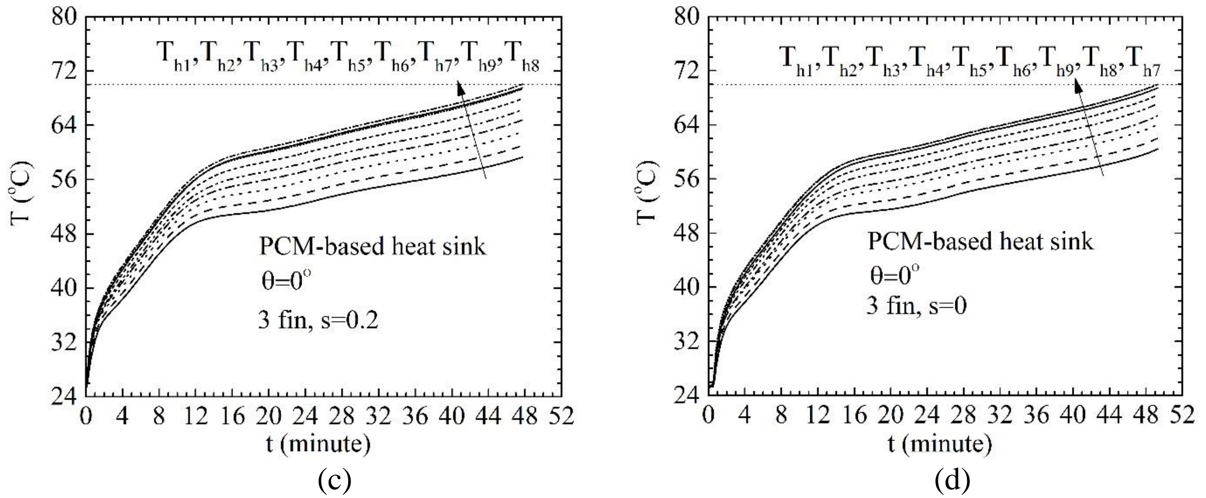

Figure 10. Time history of the heat sink base temperature: (a) s=1[42], (b) s=0.5, (c) s=0.2, (d) s=0.

3.3-Solid-liquid interface tracking

The transient solid-liquid interface tracking is photographed through side (Figure 12) and bottom (Figure 13) surfaces to better understand the melting phenomenon of PCM for different fin width ratios. The last photographs of melting tracking illustrate the progression at the moment when the critical temperature point reaches the critical operating temperature of 70 °C of the electronic component.

In the early stage (t = 6 mins), the solid-liquid interface progresses relatively uniform through the hot/heated surface for all fin configurations in Figure 12a-d. In this period, the buoyancy forces are weak to overcome the viscous forces depending on the thin melting layer adjacent to the base plate and fins. This makes conduction the dominant heat transfer mechanism. As time progresses (t=12 mins), the liquid PCM layer increases and the buoyancy force overcomes the retarding effect of viscous force. Hence, the hot liquid PCM closer to the heated wall ascends, and the cold liquid PCM descends making a counter-clockwise circulating current. This circulation results in stronger natural convection, which accelerates the phase transition rate and changes the form of the solid-liquid interface. As seen from Figure 12a-d (t = 12 mins), the solid-liquid interface gets a slightly concave shape at the upper part of the PCM medium in terms of melting convection while it gets a smooth form in the lower part. In order to avoid repetition, more details on natural convection in liquid PCM can be found in [42]. As the time elapses (t = 24 mins), the liquid fraction increases. As the liquid layer gets thicker, the dominant heat transfer mechanism starts to turn to melting convection, especially, in the upper region of the PCM medium (Figure 12a-d). This results in a higher solid-liquid interface moving rate at the upper half of the PCM medium. However, it is seen that the decreasing fin s values present appreciable changes on the solid/liquid interface shape (Figure 12b-d, t=>24 mins). Lower s values illustrate decreasing melting rate in the upper region and increasing melting rate at the lower part of the PCM enclosure. It means that melting convection is expanded to the lower region of the PCM medium and enhanced conduction heat transfer in the lower region. The effect of s on the melting interface on the

melting interface is more clear at the time step of t = 36 mins. It is seen that a concave melting interface shape is observed in the middle part of the solid PCM for decreasing s values, while a convex melting form is present in the upper region of the solid part of the PCM. This is result of enhanced heat transfer rate and increased melting rate at the lower part of the enclosure via enhanced conduction with lower s values. At the final stage of heat load, for the fin width value of s = 0, a significant part of the solid PCM completes the solid-liquid phase transition. This means s = 0 offers the highest contribution to latent heat storage potential with uniform melting behaviour, uniform temperature profile for both PCM in medium and on heat sink base and therefore longer reliable operating times. Moreover, the affect of downward increased heat transfer surface area is diminishing at the region of solid-liquid phase change completed. Thicker solid pcm region is seen at the fin tip in bottom (Figure 12, at the final stage). This is result of low thermal conductive of paraffin.

Solid-liquid interface tracking photographs obtained from the bottom surface are presented in Figure 13. Here, it is seen that the solid-liquid interface is moving faster for lower fin width ratio values. This is explained by the contribution of the downward extended heat transfer surface areas. It should be noted that the main heat transfer mechanism is conduction at the bottom of the enclosure.

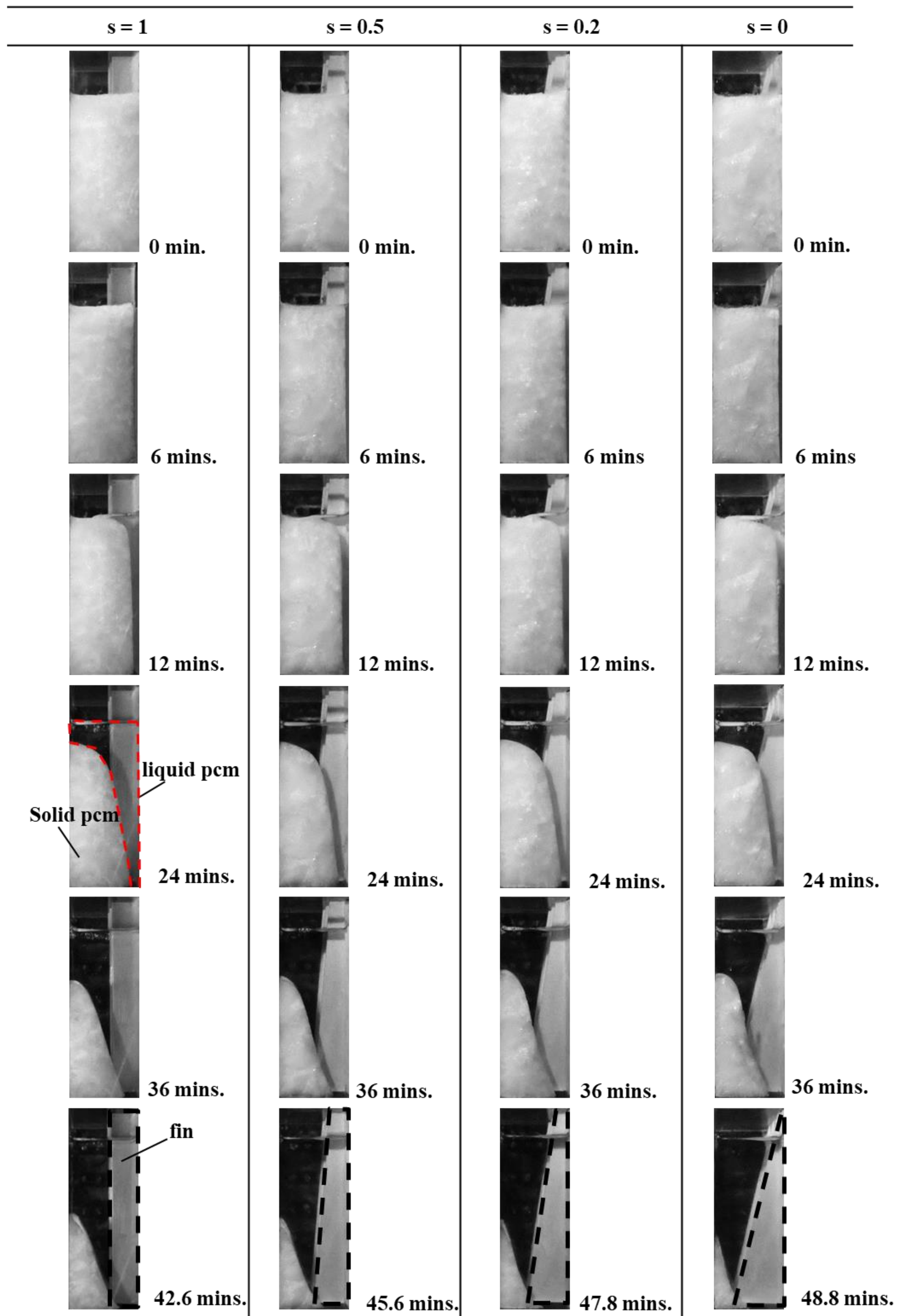

Figure 12. Side view of transient solid-liquid interface tracking for different fin length ratio (s): (a) s=1 [42], (b) s=0.5, (c) s=0.2, (d) s=0.

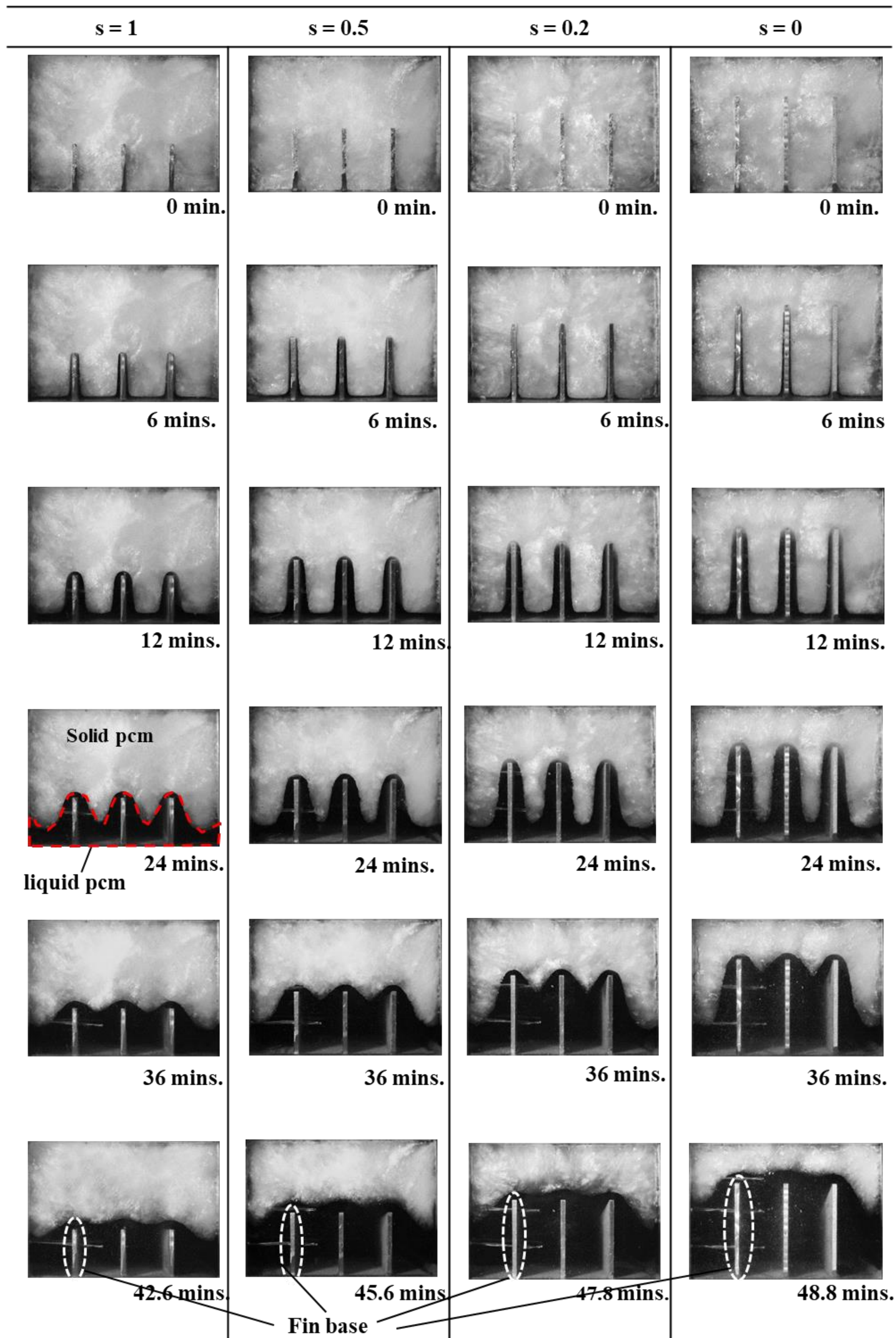

Figure 13 Bottom view of transient solid-liquid interface tracking for different fin length ratio (s): (a) s=1 [42], (b) s=0.5, (c) s=0.2, (d) s=0.

3.4-The thermal performance evaluation of the fin-based heat sink with PCM: reliable operating time (t), enhancement ratio (Ɛ) and thermal conductivity (G)

Thermal performance evaluations of different fin width ratio (s) values are presented in Figures 14-17. Transient temperature profiles of the critical points on the heat sink base for different s values are given comparatively in Figure 14. A lower temperature profile is observed on the heat sink base with decreasing values of s = 1, 0.5, 0.2 and 0, respectively (Figure 14). It shows that the temperature rising rate is diminished by lower s values. Hence, this results in prolonged reliable operating time, which is a moment to reach the critical/limit temperature value of 70 °C for lower fin width ratio values. It is seen from Figure 15a that the time to reach the limit temperature is a function of the fin width ratio. The reliable operating time is increased by 15% for s=0 compared to s=1. The enhancement ratio is also presented comparatively to illustrate the thermal performance of different s ratios in dimensionless form (Figure 15b), which is defined as

$$\mathcal{E} = t/t_{referance} \quad (1)$$

Where, t is the time to reach limit temperature for s values. Reference refers to s=1.

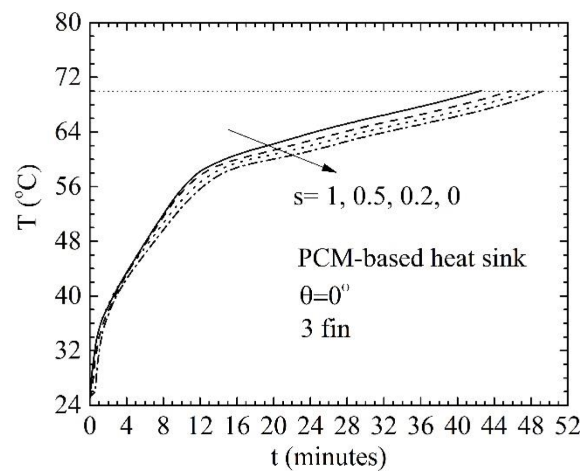

Figure 14. Transient temperature profiles of the critical points on the heat sink base.

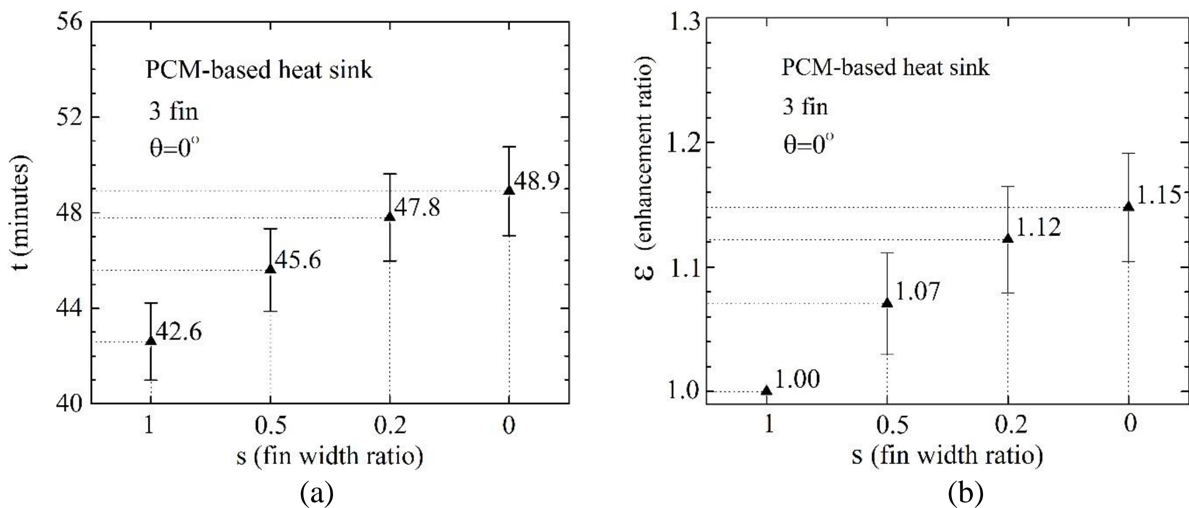

Figure 15. The effect of s values on (a) reliable operating time, and (b) enhancement ratio.

Another approach to illustrate the thermal performance of fin-based heat sink with PCM is thermal conductance, G, in Figure 16. G refers to the level of heat transferred to the PCM medium. Mathematically G of the body is given by as:

$$G = (P - P_{loss})/(T_{limit} - T_{PCM\ medium}) \quad (2)$$

Where, P and P_{loss} represent heating power and heat loss respectively; T_{limit} and T_{PCM} represent the limit operating temperature of 70 °C and average PCM medium temperature, respectively. It is shown that the thermal conductance of the body of s=0 is 38% greater compared to that of the conventional plate-fin geometry (s=1). It should be emphasized that the thermal performance of fin-based heat sink with PCM is improved significantly by a new fin design approach with the same total heat transfer surface area considering the melting phenomenon.

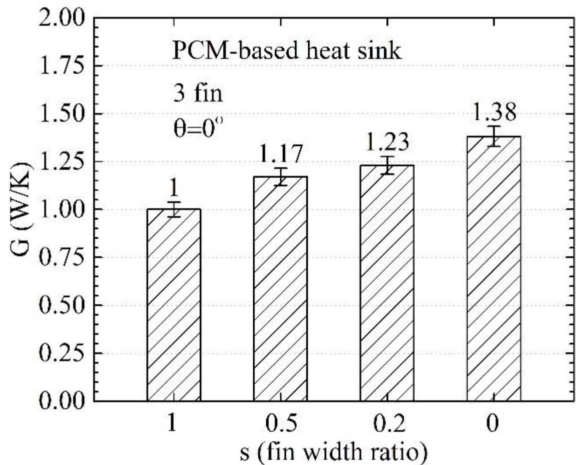

Figure 16. The effect of s values on the thermal conductance of the fin-based heat sink with PCM.

Moreover, almost the same reliable operating time is achieved with 3-fins and s=0 (t=49 minutes) compared to the 5-fins heat sink case with s=1 (t = 49.4 mins) reported in the previous study [38]. It means that the same reliable operating time is achieved with a lower heat transfer surface area. This provides lower fin quantities for similar PCM-based heat sink systems and so more lightweight and lower cost (lower manufacturing time and lower mass).

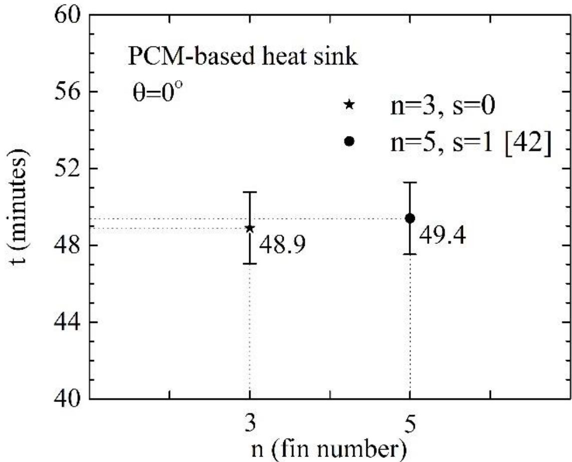

Figure 17. Comparison of the proposed fin design with the previous study [42].

Conclusions

The present experimental study explores the parametric investigation of a plate fin-based heat sink with PCM by testing different fin width ratios of s=1, 0.5, 0.2, and 0 for electronics' thermal management. The effect of fin width ratio is examined through time-dependent temperature profile (t) both base and PCM medium, melting interface visualization, enhancement ratio (ε) and thermal conductance (G). The following specific conclusions can be drawn:

1. More uniform melting behaviour, more uniform temperature profile (PCM medium and heat sink base) and longer reliable operating times are achieved with decreasing of fin width ratio (s) considering the melting phenomenon.
2. The temperature gradient in the PCM medium is reduced by 52% for s=0 in comparison to the conventional plate fin (s = 1) depending on the enhanced heat conduction mechanism and the expansion of the convection cells in the downward direction.
3. The maximum reduction in heat sink base temperature obtained was 4.5% with s=0 compared to the conventional plate fin of s = 1
4. The temperature gradient on the heat sink base is reduced by 9% for s = 0 compared to s = 1.
5. The solid-liquid interface tracking photographs illustrate the highest contribution to latent heat storage potential with more uniform melting behaviour is by the lowest s = 0 value.
6. The enhancement ratio over operating time increases 15% for s = 0 in comparison to s = 1.
7. Thermal conductance of the fin-based heat sink with PCM is greater by 38% for s = 0 compared to the conventional plate-fin geometry (s = 1).
8. Almost the same reliable operating time is achieved with 3-fins and s = 0 (t = 49 mins) compared to the conventional (s=1) 5-fins heat sink case (t = 49.4 mins) reported in the previous study.

REFERENCES

[1] S.S. Anandan, V. Ramalingam, Thermal management of electronics: a review of literature, Thermal Sci. 12 (2008) 5–26.

[2] S.M.S. Murshed, C.A.N. Castro, A Critical Review of traditional and emerging techniques and fluids for electronics cooling, Renew. Sust. Energy Rev. 78 (2017) 821–833.

[3] Z. He, Y. Yan, Z.Zhang, Thermal management and temperature uniformity enhancement of electronic devices by micro heat sinks: A review, Energy, 216 (2021) 119223

[4] Z. Zhang, X. Wang, Y. Yan, A review of the state-of-the-art in electronic cooling, e-Prime - Advances in Electrical Engineering, Electronics and Energy, 1 (2021) 100009

[5] T.D. Swanson, G.C. Birur, NASA thermal control technologies for robotic spacecraft, Appl. Therm. Eng., 23 (2003), pp. 1055-1065

[6] C.R. Raj, S. Suresh, V.K. Singh, R.R. Bhavsar, M.V.C.S. Vasudevan, V. Archita, Experimental investigation on nanoalloy enhanced layered perovskite PCM tamped in a tapered triangular heat sink for satellite avionics thermal management, Int. J. Therm. Sci., 167 (2021) 107007,

[7] D.C. Price, A review of selected thermal management solutions electronics for military system, IEEE Trans. Compon. Pack. Technol., 26 (2003) 26-39

[8] R. Kumar, M.K. Misra, R. Kumar, D. Gupta, P.K. Sharma, B.B. Tak, S.R. Meena, Phase change materials: Technology status and potential defence application, Def. Sci. J., 61 (2011), pp. 576-582

[9] S. H. Kim, C. S.Heua, J. Y.Mok, S.Kang, D.R. Kima, Enhanced thermal performance of phase change material-integrated fin-type heat sinks for high power electronics cooling, International Journal of Heat and Mass Transfer, 184 (2022) 122257

[10] H. Liu, Z. Wei, W. He, J. Zhao, Thermal issues about Li-ion batteries and recent progress in battery thermal management systems: a review, Energy Convers. Manag., 150 (2017) 304-330

[11] M.Y. Yazici, The effect of a new design preheating unit integrated to graphite matrix composite with phase change battery thermal management in low-temperature environment: an experimental study, Thermal Science and Engineering Progress 29 (2022), 101244.

[12] J. Ye, S. Mo, L. Jia, Y. Chen, Experimental performance of a LED thermal management system with suspended microencapsulated phase change material, Applied Thermal Engineering, 207 (2022) 18155.

[13] A. Karthick, P. Ramanan, A. Ghosh, B. Stalin, R.V. Kumar, I. Baranilingesan, Performance enhancement of copper indium diselenide photovoltaic module using inorganic phase change material, Asia-Pac J Chem Eng.,15 (2020) e2480.

[14] A. Karthick, K.K. Murugavel, A. Ghosh, K. Sudhakar, P. Ramanan, Investigation of a binary eutectic mixture of phase change material for building integrated photovoltaic (BIPV) system, Solar Energy Materials and Solar Cells, 207 (2020), 110360.

[15] A.R.Abdulmunem, P. M.Samin, H. A. Rahman, H. A.Hussien, I. I. Mazali, H. Ghazali, Numerical and experimental analysis of the tilt angle's effects on the characteristics of the melting process of PCM-based as PV cell's backside heat sink, Renewable Energy 173 (2021) 520-530

[16] M. Hodes, R.D. Weinstein, S.J. Pence, J.M. Piccini, L. Manzione, C. Chen, Transient thermal management of handset using phase change material (PCM), J. Electron. Packag., 124 (2002) 419-426.

[17] S. Wonorahardjo, I. M.Sutjahja, E. Tunçbilek, R. A. Achsani, M. Arıcı, N. Rahmah, PCM-based passive air conditioner in urban houses for the tropical climates: An experimental analysis on the stratum air circulation, Building and Environment, 192 (2021) 107632

[18] X. Wang, W. Li, Z.Luo, K. Wang, S.P.Shah, A critical review on phase change materials (PCM) for sustainable and energy efficient building: Design, characteristic, performance and application, Energy and Buildings, 260 (2022) 111923.

[19] N. Sarier, E. Onder Organic phase change materials and their textile applications: an overview Thermochim. Acta, 540 (2012) 7-60. 10.1016/j.tca.2012.04.013

[20] M. Kenisarin, K. Mahkamov, Solar energy storage using phase change materials, Renew. Sust. Energ. Rev., 11 (2007) 1913-1965, 10.1016/j.rser.2006.05.005

[21] M. Y. Yazici, M. Avcı, O. Aydın, M. Akgun, Effect of eccentricity on melting behavior of paraffin in a horizontal tube-in-shell storage unit: an experimental study, Sol. Energy 101 (2014) 291–298.

[22] O. Aydin, M. Avci, M.Y. Yazici, M. Akgun, Enhancing storage performance in a tube-in shell storage unit by attaching a conducting fin to the bottom of the tube, Isı Bilimi ve Teknigi Dergisi-J. Therm. Sci. Technol. 38 (2018) 1–13.

[23] W. Hua, L. Zhang, X. Zhang, Research on passive cooling of electronic chips based on PCM: A review, Journal of Molecular Liquids 340 (2021) 117183.

[24] S.K. Sahoo, M.K. Das, P. Rath, Application of TCE - PCM based heat sink for cooling of electronic components: A review, Renew. Sust. Energy Rev. 59 (2016) 550–582.

[25] M.Y. Yazici., M. Saglam, M., Avci, O. Aydin, Thermal energy storage performance of PCM/graphite matrix composite in a tube-in-shell geometry, Thermal Science and Engineering Progress 23 (2021) 100915.

[26] Arshad, A., Jabbal, M., Faraji, H., Talebizadehsardari, P., Bashir, M. A., Yan, Y.. Thermal performance of a phase change material-based heat sink in presence of nanoparticles and metal-foam to enhance cooling performance of electronics. Journal of Energy Storage 48 (2022) 103882.

[27] A.R.Abdulmunem, P. M.Samin, H. A. Rahman, H. A.Hussien, I. I. Mazali, Enhancing PV Cell's electrical efficiency using phase change material with copper foam matrix and multi-walled carbon nanotubes as passive cooling method, Renewable Energy 60 (2020) 663-675.

[28] K.C. Nayak, S.K. Saha, K. Srinivasan, P. Dutta, A numerical model for heat sinks with phase change materials and thermal conductivity enhancers, Int. J. Heat Mass Transfer 49 (2006) 1833–1844.

[29] R. Kandasamy, X.C. Wang, A.S. Mujumdar, Transient cooling of electronics using phase change material (PCM)-based heat sinks, Appl. Therm. Eng. 28 (2008) 1047–1057.

[30] S.K. Saha, P. Dutta, Heat transfer correlations for PCM-based heat sinks with plate fins, Appl. Therm. Eng. 30 (2010) 2485–2491.

[31] S.C. Fok, W. Shen, F.L. Tan, Cooling of portable hand-held electronic devices using phase change materials in finned heat sinks, Int. J. Therm. Sci. 49 (2010) 109–117.

[32] S.F. Hosseinizadeh, F.L. Tan, S.M. Moosania, Experimental and numerical studies on performance of PCM-based heat sink with different configurations of internal fins, Appl. Therm. Eng. 31 (2011) 3827–3838.

[33] S. Mahmoud, A. Tang, C. Toh, R. Al-Dadah, S.L. Soo, Experimental investigation of inserts configurations and pcm type on the thermal performance of PCM based heat sinks, Appl. Energy 112 (2013) 1349–1356.

[34] R. Baby, C. Balaji, Experimental investigations on phase change material based finned heat sinks for electronic equipment cooling, Int. J. Heat Mass Transfer 55 (2012) 1642–1649

[35] S. Gharbi, S. Harmand, S.B. Jabrallah, Experimental comparison between different configurations of PCM based heat sinks for cooling electronics components, Appl. Therm. Eng. 87 (2015) 454–462

[36] M.J. Ashraf, H.M. Ali, H. Usman, A. Arshad, Experimental passive electronics cooling: parametric investigation of pin-fin geometries and efficient phase change materials, Int. J. Heat Mass Transfer 115 (2017) 251–263.

[37] A. Arshad, H.M. Ali, M. Ali, S. Manzoor, Thermal performance of phase change material (PCM) based pin-finned heat sinks for electronic devices: effect of pin thickness and PCM volume fraction, Appl. Therm. Eng. 112 (2017) 143–155.

[38] A. Arshad, H.M. Ali, W. Yan, A.K. Hussein, M. Ahmadlouydarab, An experimental study of enhanced heat sinks for thermal management using n-eicosane as phase change material, Appl. Therm. Eng. 132 (2018) 52–66.

[39] A. Arshad, H.M. Ali, S. Khushnood, M. Jabbal, Experimental investigation of PCM based round pin fin heat sinks for thermal management of electronics: effect of pin-fin diameter, Int. J. Heat Mass Transfer 117 (2018) 861–872.

[40] H.M. Ali, M.J. Ashraf, A. Giovannelli, M. Irfan, T. Irshad, H.M. Hamid, F. Hassan, A. Arshad, Thermal management of electronics: an experimental analysis of triangular, rectangular and pin-fin heat sinks for various PCMs, Int. J. Heat Mass Transfer 123 (2018) 272–284.

[41] H.M. Ali, A. Arshad, Experimental investigation of n-eicosane based circular pin-fin heat sinks for passive cooling electronic devices, Int. J. Heat Mass Transfer 112 (2017) 649–661.

[42] M. Y. Yazici, M. Avci, O. Aydin, Combined effects of inclination angle and fin number on thermal performance of a PCM-based heat sink, Applied Thermal Engineering, 159 (2019) 113956

[43] J. Xie, K. FahChoo, J. Xiang, H. M.M. Lee, Characterization of natural convection in a PCM-based heat sink with novel conductive structures, International Communications in Heat and Mass Transfer, 108 (2019) 104306.

[44] J.Y.Ho, Y.S.See, K.C.Leong, T.N.Wong, An experimental investigation of a PCM-based heat sink enhanced with a topology-optimized tree-like structure, Energy Conversion and Management 245(2021) 114608.

[45] K. Dammak, A. Hami, Thermal reliability-based design optimization using Kriging model of PCM based pin fin heat sink, International Journal of Heat and Mass Transfer, 166(2021) 120745

[46] A.Arshad, M. Jabbal, P. T. Sardari, M. A. Bashir, H. Faraji, Y. Yan, Transient simulation of finned heat sinks embedded with PCM for electronics cooling, Thermal Science and Engineering Progress 18 (2020), 100520

[47] A. Arshad, M.I. Alabdullatif, M. Jabbal, Y. Yan, Towards the thermal management of electronic devices: A parametric investigation of finned heat sink filled with PCM, International Communications in Heat and Mass Transfer 129 (2021) 105643

[48] R. Kalbasi, Introducing a novel heat sink comprising PCM and air - Adapted to electronic device thermal management, International Journal of Heat and Mass Transfer 169 (2021) 120914.

[49] R. Kothari, S. K.Sahu, S.I. Kundalwal, Investigation on thermal characteristics of nano enhanced phase change material based finned and unfinned heat sinks for thermal management system, Chemical Engineering and Processing - Process Intensification, 162 (2021) 108328.

[50] C.R. Raj, S.Suresh, S. Vasudevan, M.Chandrasekar, V.K. Singh, R.R.Bhavsard, Thermal performance of nano-enriched form-stable PCM implanted in a pin finned wall-less heat sink for thermal management application, Energy Conversion and Management 226 (2020) 113466

[51] J. H. Jeong, S. Hah, D. Kim, J. H. Lee, S. M. Kim, Thermal analysis of cylindrical heat sinks filled with phase change material for high-power transient cooling, International Journal of Heat and Mass Transfer, 154 (2020) 119725.

[52] A. N.Desai, A. Gunjal, V.K.Singhc, Numerical investigations of fin efficacy for phase change material (PCM) based thermal control module, International Journal of Heat and Mass Transfer, 147 (2020) 118855

[53] A. N.Desai, H.Shah, V.K.Singh, Novel inverted fin configurations for enhancing the thermal performance of PCM based thermal control unit: A numerical study, Applied Thermal Engineering, 195 (2021) 117155 - area augmentation

[54] S.Al-Omari, Z. A. Qureshi, F. Mahmoud, E. Elnajjar, Thermal management characteristics of a counter-intuitive finned heat sink incorporating detached fins impregnated with a high thermal conductivity-low melting point PCM, International Journal of Thermal Sciences, 175 (2022) 107396

[55] R. Hemati, F. Veysi, A. Qaderi, Experimental investigation of the simultaneous effect of using phase change material/plate-fin heat sink on thermal performance of a power supply unit, Sustainable Energy Technologies and Assessments, 52 (2022) 102009

[56] A. Arshad, M. Jabbal, Y. Yan, J. Darkwa, The micro-/nano-PCMs for thermal energy storage systems: a state of art review, International Journal of Energy Research, 43 (2019) 5572-5620.

[57] aalco, UK6082 - T6~T651 plate properties datasheet. https://www.aalco.co.uk/datasheets/Aluminium-Alloy_6082-T6~T651_148.ashx, 2019 (accessed 18 January 2023)